MEDWIN PUBLISHERS
Committed to create value for Researchers

Physical Science & Biophysics Journal
ISSN: 2641-9165

Layered Hybrid of Molybdenum (VI)-Oxide Based On Electron-Rich Phenanthroline Organic Linkers

Chong SV[1,2,*], U-din I[3], and Tallon JL[1,2]

[1]Robinson Research Institute, Victoria University of Wellington, PO Box 33436, Lower Hutt 5046, New Zealand

[2]MacDiarmid Institute for Advanced Materials and Nanotechnology, Victoria University of Wellington, PO Box 600 Wellington 6140, New Zealand

[3]Institute of Fundamental Sciences, Massey University, Private Bag 11222 Palmerston North 4442, New Zealand

Research Article

Volume 1 Issue 1

Received Date: March 01, 2017

Published Date: March 08, 2017

DOI: 10.23880/psbj-16000101

Corresponding author: Shen V Chong, Robinson Research Institute, Victoria University of Wellington, Address: PO Box 33436 Lower Hutt New Zealand, Tel: 04-4630072; E-mail: shen.chong@vuw.ac.nz

Abstract

We have prepared three-dimensional framework of covalently bonded layers of inorganic oxide containing molybdenum interlinked by electron-rich organic ligands. The structure of MoO_3-(3,8-phenanthroline)0.5 consists of corner-sharing of {MoO_5N} octahedra. Raman spectra correlate very well to the structural data and illustrate the subtle choice of the ligands used can affect the vibration characteristics of the Mo-O bonds. Magnetization measurements indicate the susceptibility only changes slightly with temperature in the high-temperature region above 50 K, an indication of a Pauli paramagnetic metallic behaviour. The increase in the electronic density-of-state due to the electron-rich organic spacer is further confirmed by heat capacity measurement on pressed pellet samples where the electronic specific heat, γ, is much higher as compared to the bipyridyl counterpart.

Keywords: Organic-inorganic hybrids; Phenanthroline; Polycyclic Aromatic Hydrocarbons; Molybdenum oxide

Introduction

Low dimensional organic-inorganic layered materials have displayed many potential applications in catalysis, sorption, separation and photochemistry [1-5]. However, most of the organic spacer molecules used in these hybrids are either electrical insulators or poor conductors. For molybdenum-oxide based layered hybrids, the organic spacers used include alkyl amines [6-9], and more electron-rich pyridine [9-11], pyrazine [10,12], bipyridines [10,11,13,14] and other five-member heterocyclic ring aromatics [9,15]. Solid-state polycyclic aromatic hydrocarbons (PAHs) especially [*n*]phenancene with zigzag fusion of *n*-number of benzene rings and other non-linear PAHs have come under the spotlight in recent years owing to the realization of exotic electronic property such as superconductivity [16-19]. Phenanthroline, which contains three fused benzene rings, is more electron-rich compared to the other aromatic ligand systems stated above, therefore might

offer untapped diverse electronic, magnetic and chemical properties. Moreover, it is a well-known chelating agent in making organ metallic complexes [20,21], and forms hybrids with molybdenum-oxides readily either covalently bonded to the molybdate clusters (4,7-phenanthroline) [22] or non-covalently intercalated in between α-MoO_3 layers. An example of the latter is where the 1,10-phenanthroline orient either perpendicular or parallel to the oxide layers [23].

Here we report using 3,8-phenanthroline (phen), an analogue of phenanthrene, by replacing the two apical carbons with nitrogen, as covalent-bond linking molecules in molybdenum-oxide-based hybrid material. The use of electron-rich moieties and the direct bonding onto the inorganic layers would facilitate the direct injection of electrons into the metal oxide layers or assist in the interlayer transfer of charge carriers. To the best of our knowledge, there are no reports of 3, 8-phenanthroline being used as a covalent linker between any two-dimensional metal-oxide layers.

Materials and Methods

MoO_3-(3,8-phenanthroline)$_{0.5}$, herein denotes as MoO_3-phen, was prepared via hydrothermal reaction of MoO_3, 3,8-phenanthroline (Chemveda Life Sciences) and H_2O using a molar ratio of 0.28:0.095:277 mM. The reactants were kept in a sealed Teflon-lined stainless-steel autoclave reactor at 160-170 °C for 70 hours before slowly cooling (approximately -10 °C per hour) the autoclave to room temperature inside the oven. Dark green platelet crystals of sizes *ca.* 40 × 100 μm were obtained upon filtration. Elemental analysis shows calculated C = 30.72 %, H =1.72 %, N = 5.99 %; experimental values gave C = 28.50 %, H = 1.70 %, N = 5.45%.

All measurements were carried out on the as-filtered product. Single-crystal x-ray diffraction measurements were performed with a Rigaku-Spider X-ray diffractometer with a wrap-around image-plate detector and three-axis kappa goniostat that uses Cu K_α (λ = 1.5428 Å) as the probing radiation. Raman spectra were recorded with a Jobin-Yvon LabRam Raman microscope system using excitation of 633 nm and 2-3 mW at the sample. Magnetic susceptibility measurements were performed using a Quantum Design MPMS XL magnetometer. Heat capacity measurements were performed on pressed pellet samples of the hybrids on a Quantum Design PPMS in zero applied magnetic field.

Results and discussion

Single Crystal X-ray Diffraction

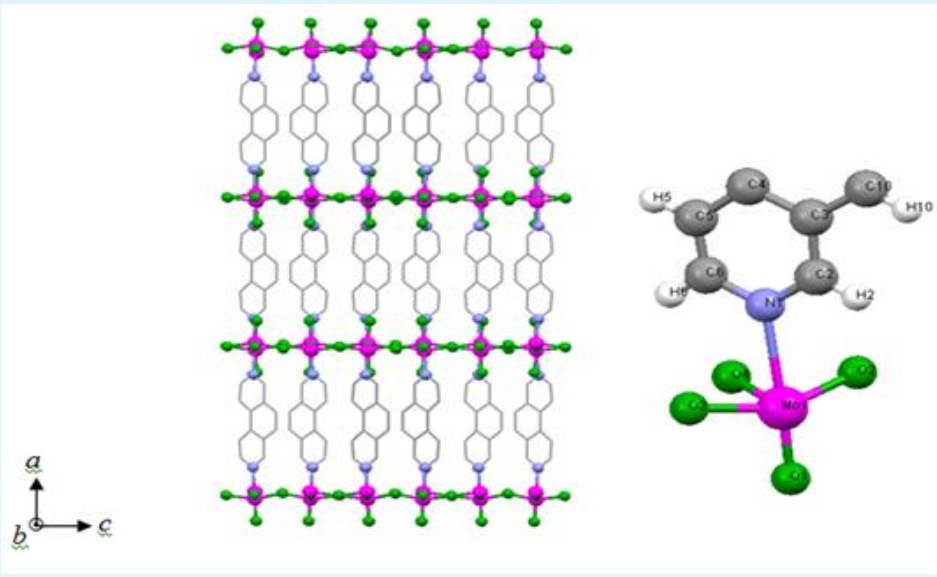

Figure 1: 3D crystal structure (left) and repeat unit of MoO_3-phen (right).

MoO_3-phen belongs to the *Cmca* space group. Octahedral {MoO_5N} moieties are corner-shared to give ragged layers of {MoO_4} in the *bc*-plane. These inorganic layers are bridged through phen ligands that coordinate axially to metal atoms to form three-dimensional (3D) networks of layered organic-inorganic hybrid (Figure 1). The crystal structure of MoO_3-phen closely resembles its bipyridyl (bpy) counterpart, MoO_3-(4,4′-bipyridyl)$_{0.5}$ (herein denotes as MoO_3-bpy) [10,13]. The octahedral coordination geometry at each metal atom site of MoO_3-phenanthroline is defined by one terminal oxo group, four equatorial oxo groups and a nitrogen donor arising from the phenanthroline ligand.

The strong influence of the terminal oxo groups is reflected in long Mo(1)-N(1) (2.419(11) Å) bond distances, while the terminal oxo bond length, Mo(1)=O(1) (1.699(9) Å), and bridging oxo bond lengths, which range from 1.776 Å to 1.883 Å, are within the expected values for molybdenum oxides [13,24,25]. The bridging oxygen bonds, Mo(1)-O(4)-Mo(1), run almost parallel to the short *b*-axis and are nearly linear with Mo(1)-O(4)-Mo(1) and O(4)-Mo(1)-O(4) angles of 179.1(3)^o and 164.4(4)^o, respectively. The remaining bridging oxygen bonds, Mo(1)-O(2)-Mo(1) and Mo(1)-O(3)-Mo(1), are approximately parallel to the longer *c*-axis and are non-linear with their respective angles of 153.1(8)^o and 163.8(9)^o. The axial (Mo=O) and metal-ligand (Mo-N) bonds alternate in direction, which is approximately parallel to the long *a* axis, leading to undulating {MoO_4} layers in the *bc* plane. Key refinement details are summarized in Table 1. Selected bond lengths/angles for MoO_3-phen are summarized in Table S1 in Supporting Information.

The crystal structures of MoO_3-phen and its bipyridyl analogue [13] share a similar ragged layered structure. In the latter, however, the molybdenum-oxide layer lies in the *ab* plane and Mo-O-Mo angles ranges from 156.4° to 169.8^o. However, the packing of organic legends in these compounds is distinctly different: π-stacking for phenanthroline in MoO_3-phen involves only the central phenyl group of the phenanthroline ligand, whereas there is no π-stacking of the bipyridyl molecules in MoO_3-bpy. For MoO_3-phen, there is also a staggered herring-bone alignment of edge-to-face contacts, whereas for MoO_3-bpy there is only an orthogonal alignment of legends. Therefore, the cages defined by MoO_3-phen are much smaller than those formed in MoO_3-bpy which limits the possibilities of introducing even very small metal atoms/ions there.

From the above single-crystal structural refinement of the nearest-neighbor bond distances we calculated the bond valence sums, $V_{Mo} = \Sigma_i \exp[(r_0 - r_i)/0.37]$ [26,27], for the six-coordinated site to be V_{Mo} = 6.23. In comparison, the value of V_{Mo} for MoO_3-bpy [13], ranges from 6.17 to 6.21, which is similar to our MoO_3-phen. We conclude that the mean valence of Mo in MoO_3-phen should be 6+.

Parameter	MoO_3-(3,8 Phenanthroline)$_{0.5}$
a (/Å)	22.7233(4)
b (/Å)	7.7355(10)
c (/Å)	14.5903(10)
α, β, γ(°)	90, 90,90
V (/Å^3)	2564.63(18)
Crystal system	Orthorhombic
Space group	*Cmca*
Data range (/Å)	20-0.81
Completeness (/%)	99
Redundancy	12.48
R_{int}, R_{sigma} (/%)	9.89, 5.43
Asymm. unit	$MoO_3C_6H_4N$
*R*1(obs), #data*	0.0548, 651
*R*1(all), #data	0.0615, 804
*wR*2 (all data)	0.1751
Resid. Density	1.30, -1.72
*I>2s(I)	

Table 1: Selected crystallographic and refinement details of MoO_3-phen.

Based on the above structural analysis it can be said that phenanthroline (or phenancene-like molecules) can potentially offer the same structural diversity as the other orgnaic spacer molecules. Variuos experimental techniques can be used to further understand the influence of this ligand on the electronic and physical propertries of layered hybrid networks. We present below the Raman spectroscopy measurements, followed by magnetisation and heat capacity study.

Raman Spectroscopy

The Raman spectrum of MoO_3-phen as shown in Figure 2 can be divided into two spectral regions. In the first region, that spans 450-1000 cm^{-1}, four distinct bands can be observed. The first significant Raman scattering band occurs at 662 cm^{-1}, and two strong bands at 754 and 815 cm^{-1} are identified as stretching vibrations of bridging oxygen's in the Mo-O-Mo entity [24]. However, positions of these modes are significantly shifted for MoO_3-phen

when compared with MoO_3-bpy (Figure2), most likely due to differences in the equatorial bridging bond angles for these two compounds. For example, for MoO_3-phen [O(3)–Mo(1)–O(4)] =96.37° and for MoO_3-bpy [O(1)–Mo(1)–O(2)] = 100.2° [13]. Generally, in molybdenum-oxide systems, the terminal oxo groups, Mo=O are characterized by narrow Raman bands between 900-1000 cm^{-1} [24, 28]. Accordingly, the two Raman bands that appear at 915 cm^{-1} and 991 cm^{-1} in the Raman spectra of MoO_3-phen are assigned to stretching vibrations of terminal oxygen Mo=O. However, the Raman spectrum of MoO_3-bpy (our measurement) displays a single well-behaved band at 917 cm^{-1}. This may suggest the molybdenum-oxide octahedra are more distorted in MoO_3-phen as compared to MoO_3-bpy. Raman modes due to aromatic rings in phenanthroline appear above1000 cm^{-1}wavenumbers and are assigned to various stretching and bending vibrations caused by the aromatic rings in phenanthroline [29-31].

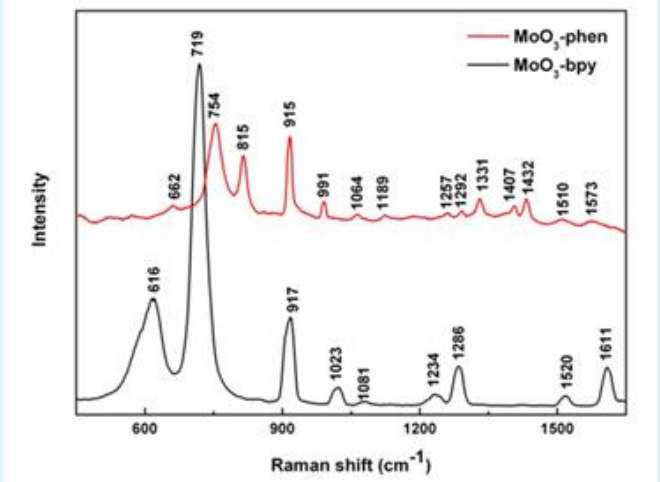

Figure 2. Raman measurements from MoO_3-phen and MoO_3-bpy powder.

Magnetic Behavior

Figure 3 shows the temperature dependence of the susceptibility of MoO_3-phen measured at high magnetic fields. Over much of the temperature range particularly above 50 K, the susceptibility of MoO_3-phen shows very weak temperature dependency. This is an indication of a metallic behaviour given by the Pauli-like temperature-independence paramagnetic behaviour. This nearly-free-electron-like metallic behaviour is most likely to be associated with the electron-rich phenanthroline tethering molecules. Just below 50 K there is a magnetic transition which is surprising given that Mo^{6+} (as given by the bond-valence sum analysis) is non-magnetic. The susceptibility then rises with Curie-Weiss behaviour below 30 K. The appearance of this low-temperature magnetic transition and the upturn is likely due to the presence of molybdenum in a lower oxidation states such as Mo^{5+} where the spin, S = ½, or S = 1 for high-spin Mo^{4+}. The dark green colour of the MoO_3-phen crystallites is an indication of the presence of reduced molybdenum species.

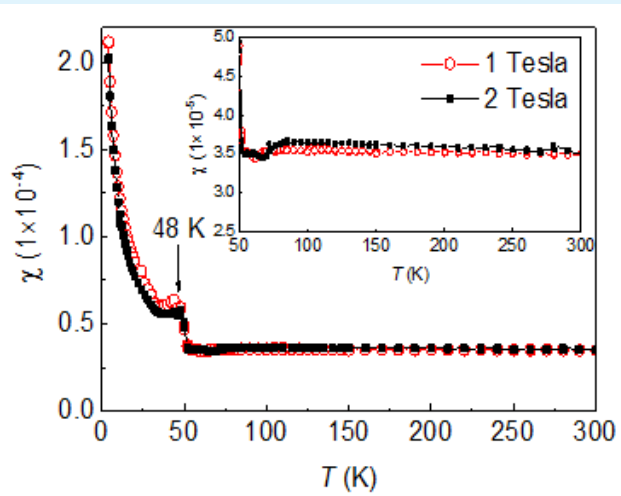

Figure 3: Temperature-dependent susceptibility measurements recorded at different applied magnetic fields - 1 and 2 Tesla. Inset shows the enlargement of the high-temperature region.

Specific Heat Capacity

In the absence of electrical transport measurements we confirm the presence of an increase in the electronic density-of-state from specific heat capacity measurements. The low-temperature specific heat, C, comprises a free carrier electronic term linear in T and a lattice (phonon) term which varies as T^3, that is, $C = \gamma T + BT^3$. A plot of C/T versus T^2 should give a linear slope with a finite non-zero intercept which is equal toγ, the electronic specific heat coefficient. Figure 4 shows such a plot giving a finite intercept with γ = 1.3 mJ/(mol·K^2). Notice that this value is higher than that of MoO_3-bpy (γ = 0.9 mJ/(mol·K^2)) but closer to the γ value of metallic H_xMoO_3-$(bpy)_{0.5}$[13] (γ = 1.6 mJ/(mol·K^2)), which we have measured under the same conditions (see Figure S1, Supporting Information). Taken along with the magnetic data, both these results strongly support the presence of free carriers in this material.

This opens the important question to how the phase diagram will evolves with further doping, and what other correlated states might be found in these, and related, systems.

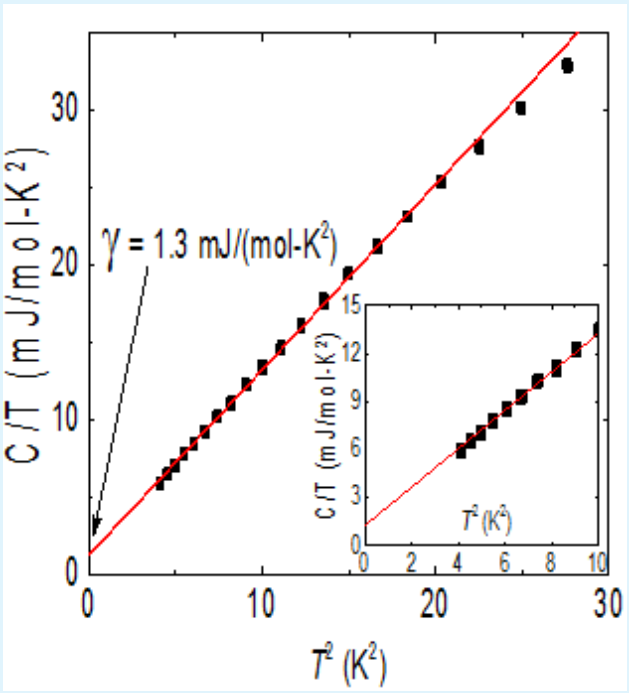

Figure 4: Low-temperature region of the zero field specific heat of a pressed pellet sample of MoO_3-phen.

Conclusions

Hydrothermal synthesis has been used to prepare layered organic-inorganic hybrid material containing molybdenum-oxide and (3, 8) phenanthroline for the first time. In MoO_3-(phenanthroline)$_{0.5}$ (or MoO_3-(phen)) the inorganic layer consists of corner-shared {MoO_5N}octahedra with ragged layers of {MoO_4} in the basal plane. Raman spectroscopy shows that the {MoO_5N} octahedral in MoO_3-phen are more distorted than those in MoO_3-bpy with the presence of two Mo=O bands. Magnetic measurements show that MoO_3-phen exhibits very weak magnetism at high-temperature and a Pauli-like temperature-independent susceptibility - an evidence of the presence of free carriers and self-doping. This is supported by a non-zero electronic specific heat coefficient and a value that is close to that of the metallic hydrogen doped H_xMoO_3-(bpy)$_{0.5}$.

Competing interests

The authors declare that they have no competing interests.

Author's contribution

All authors made equally valuable contributions to this paper. All authors read and approved the final manuscript. All the experimental work which Islah-u-din has done was carried out at Massey University, New Zealand.

Additional file

Supporting Information: Heat capacity measurements; and selected bond lengths and angles.

Acknowledgements

We acknowledge funding support from the Marsden Fund of New Zealand (grant IRL0501) and from the MacDiarmid Institute for Advanced Materials and Nanotechnology for the Spider X-ray detector and for research support. The Higher Education Commission, Pakistan, provided a doctoral scholarship for I.U.

References

1. Pardo R, Zayat M, Levy D (2011) Photochromic organic-inorganic hybrid materials. Chem Soc Rev 40(2): 672-687.

2. Zhu T, Row KH (2012) Preparation and applications of hybrid organic-inorganic monoliths- A review. J Sep Sci 35(10-11): 1294-1302.

3. Wang Q, O'Hare D (2012) Recent advances in the synthesis and application of layered double hydroxide (LDH) nanosheets. Chem Rev 112(7): 4124-4155.

4. Zhang S, Audebert P, Wei Y, Choueiry AA, Lanty G, et al. (2010) Preparations and characterizations of luminescent two dimensional organic-inorganic perovskite semiconductors. Materials 3(5): 3385-3406.

5. Kango S, Kalia S, Celli A, Njuguna J, Habibi Y et al. (2013) Surface modification of inorganic nanoparticles for development of organic-inorganic

nanocomposites - A review. Progress in Polymer Science 38(8): 1232-1261.

6. Ayyappan S, Subbanna GN, Rao CN (1995) Novel metastable structures of WO_3, MoO_3, and $W_{1-x}Mo_xO_3$ obtained by the deintercalation of layered amine adducts. Chem Eur J 1(3): 165-170.

7. De Farias RF (2005) Molybdenum oxide as a molecular sieve towards nitrogen containing molecules: synthesis and characterization of MoO_3 intercalation compounds with nicotinamide and hexamethylenetetramine. Mater Chem Phys 90: 302-309.

8. Xu Y, Lu J, Goh NK (1999) Hydrothermal assembly and crystal structures of three novel open frameworks based on molybdenum (VI) oxides. J Mater Chem 9(7): 1599-1602.

9. Schollhorn R, Schulte-Nölle T, Steinhoff G (1980) Layered intercalation complexes of the hydrogen bronze $H_{0.5}MoO_3$ with organic lewis bases. J Less-Common Met 71(1): 71-78.

10. Zhang X, Hejaz M, Thiagarajan SJ, Woerner WR, Banerjee D, et al. (2013) From 1D chain to 3D network: a new family of inorganic-organic hybrid semiconductors $MO_3(L)_x$ (M = Mo, W; L = organic linker) built on perovskite-like structure modules. J Am Chem Soc 135: 17401-17407.

11. Johnson JW, Jacobson AJ, Rich SM, Brody JF (1981) New layered compounds with transition-metal oxide layers separated by covalently bound organic ligands. Molybdenum and tungsten trioxide-pyridine. J Am Chem Soc 103: 5246-5247.

12. De Ferias RF (2001) Synthesis and characterization of MoO_3–pyrazine hybrids. Inter J Inorg Mater 3(4-5): 303-307.

13. Hagrman PJ, La Duca RL, Koo HJ, Rarig R, Haushalter RC, et al. (2000) Ligand influences on the structures of molybdenum oxide networks. Inorg Chem 39(19): 4311-4317.

14. Zapf PJ, Haushalter RC, Zubieta J (1997) Hydrothermal synthesis and structural characterization of a series of one-dimensional organic/inorganic hybrid materials of the $[(MoO_3)_n(2,2'\text{-bipy})_m]$ family: $[MoO_3(2,2'\text{-bipy})]$, $[Mo_2O_6(2,2'\text{-bipy})]$, and $[Mo_3O_9(2,2'\text{-bipy})_2]$. Chem Mater 9: 2019-2024.

15. Itoh T, Wang J, Matsubara I, Shin W, Izu N, et al. (2008) VOCs sensing properties of layered organic–inorganic hybrid thin films: MoO_3 with various interlayer organic components. Mater Let 62(17-18): 3021-3023.

16. Wang XF, Liu RH, Gui Z, Xie YL, Yan YJ, et al. (2011) Superconductivity at 5 K in alkali-metal-doped phenanthrene. Nature Commun 2: 507.

17. Mitsuhashi R, Suzuki Y, Yamanari Y, Mitamura H, Kambe T et al. (2010) Superconductivity in alkali-metal-doped picene. Nature 464(4): 76-79.

18. Kubozono Y, Mitamura H, Lee X,He X, Yamasaki Y et al. (2011) Metal-intercalated aromatic hydrocarbons: a new class of carbon-based superconductors. PhysChemChemPhys 13(37): 16476-16493.

19. Xue M, Cao T, Wang D, Wu Y (2012) Superconductivity above 30 K in alkali-metal-doped hydrocarbon. Sci Rep 2: 389.

20. Hirohama T, Kuranuki Y, Ebina E, Sugizaki T, Arii H, et al. (2005) Copper(II) complexes of 1,10-phenanthroline-derived ligands: Studies on DNA binding properties and nuclease activity. J Inorg Biochem 99(5): 1205-1219.

21. Brandt WW, Dwyer FP, Gyarfas EC (1954) Chelate Complexes of 1,10-Phenanthroline and Related Compounds. Chem Rev 54(6): 959-1017.

22. Hagrman D, Zapf PJ, Zubieta J (1998) A two-dimensional network constructed from hexamolybdate, octamolybdate and $[Cu_3(4,7\text{-phen})_3]^{3+}$ clusters: $[\{Cu_3(4,7\text{-phen})_3\}_2\{Mo_{14}O_{45}\}]$. Chem Commun 12: 1283-1284.

23. de Farias RF, Airoldi C (2003) Some structural features of MoO_3-1,10-phenanthroline intercalation compounds. J Phys Chem Solids 64(11): 2199-2204.

24. Seguin L, Figlarz M, Cavagnat R, Lassègues JC (1995) Infrared and Raman spectra of MoO_3 molybdenum trioxides and $MoO_3{\cdot}xH_2O$ molybdenum trioxide hydrates. Spectrochim Acta 51(8): 1323-1344.

25. Figlarz M (1989) New oxides in the WO_3-MoO_3 system. Prog Solid State Chem 19(1): 1-46.

26. Brown ID, Altermatt D (1985) Bond-valence parameters obtained from a systematic analysis of the Inorganic Crystal Structure Database. Acta Cryst B 41(4): 244-247.

27. Shields GP, Raithby PR, Allen FH, Mother well WDS (2000) The assignment and validation of metal oxidation states in the Cambridge Structural Database. Acta Cryst B 56(3): 455-465.

28. Briand LE, Hirt AM, Wachs IE (2001) Quantitative determination of the number of surface active sites and the turnover frequencies for methanol oxidation over metal oxide catalysts: application to bulk metal molybdates and pure metal oxide catalysts. J Catal 202(2): 268-278.

29. Muniz-Miranda M, Pergolese B, Bigotto A (2010) SERS and DFT investigation on the adsorption of 1,10-phenanthroline on transition metal surfaces. Phys Chem Chem Phys 12(5): 1145-1151.

30. Zawada K, Bukowska J (2000) An interaction of 1,10-phenantroline with the copper electrode in neutral and acidic aqueous solutions: a surface enhanced Raman scattering study. J Mol Struct 555(1-3): 425Z.

31. Reiher M, Brehm G, Schneider S (2004) Assignment of vibrational spectra of 1,10-phenanthroline by comparison with frequencies and Raman intensities from density functional calculations Phys Chem A 108(5): 734-742.